NASA TECHNICAL MEMORANDUM

Report No. 53830

AN IMPROVED CONTROL SYSTEM FOR THE APOLLO TELESCOPE MOUNT

By M. T. Borelli

Astrionics Laboratory

April 1, 1969

NASA

George C. Marshall Space Flight Center

Marshall Space Flight Center, Alabama

1. Report No. NASA TM X-53830	2. Government Accession No.	3. Recipient's Catalog No.
4. Title and Subtitle An Improved Control System for the Apollo Telescope Mount		5. Report Date April 1, 1969
		6. Performing Organization Code MSFC-S&E-ASTR
7. Author(s) M. T. Borelli		8. Performing Organization Report No.
9. Performing Organization Name and Address Astrionics Laboratory, S&E George C. Marshall Space Flight Center Marshall Space Flight Center, Ala. 35812		10. Work Unit No.
		11. Contract or Grant No.
		13. Type of Report and Period Covered
12. Sponsoring Agency Name and Address		
		14. Sponsoring Agency Code

15. Supplementary Notes

16. Abstract

    A different method of operating the present control system for the Apollo Telescope Mount's control moment gyro is presented. This method results in a broader bandwidth for the control system and consists of modifying the double-gimbal control moment gyros to operate in a single-gimbal mode during all solar experimental periods. If the inner gimbals are used for dynamic control, then the outer gimbals would be inhibited or rigidly clamped to the frame during the experiments. Between experiments, the inhibited outer gimbals would be oriented to maximize the momentum storage capability of the system. The expected increase in bandwidth is from two to three times the present system bandwidth. Inner to outer gimbal cross coupling nonlinearities would also be eliminated during experimental periods. The H-vector control law would still be applicable for this new configuration.

17. Key Words ATM control system CMG control Spacecraft control Momentum exchange devices	18. Distribution Statement Announce in SAB

19. Security Classif. (of this report) Uncl.	20. Security Classif. (of this page) Uncl.	21. No. of Pages 18	22. Price

TABLE OF CONTENTS

LIST OF ILLUSTRATIONS

DEFINITION OF SYMBOLS

i, j	general subscripts (range 1, 2, 3)
—	bar above a letter indicates a vector quantity
$\cdot$	dot above a letter indicates a time derivative
c	$\equiv$ cosine
$G_1(p)$, $G_3(p)$	compensation networks for the inner and outer gimbal velocity servos, respectively
$G_{cc(1)}$, $G_{cc(3)}$	crossfeed compensation for the inner and outer gimbal velocity servos, respectively
H	magnitude of the momentum of the CMG's
$\overline{H}_T$	total momentum vector of the (1), (2), and (3) CMG's
$\overline{H}_{T(com)}$	time integral of the attitude control system moment command
$\overline{H}_{TE}$	error signal between $\overline{H}_{T(com)}$ and $\overline{H}_T$
$\overline{H}_{TEX}$, $\overline{H}_{TEY}$, $\overline{H}_{TEZ}$	X, Y, Z components of the $\overline{H}_{TE}$ vector
$\overline{H}_{TEiA(j)}$, $\overline{H}_{TEiB(j)}$	components of the $\overline{H}_{TE}$ vector along coordinates $\overline{1}_{1A(j)}$, $\overline{1}_{2A(j)}$, $\overline{1}_{3A(j)}$ and $\overline{1}_{1B(j)}$, $\overline{1}_{2B(j)}$, $\overline{1}_{3B(j)}$, respectively
J_1	$= J_{11} - N_g \, (1 + N_g) \, J_{MR}$
J_3	$= -1/2 \sin 2\delta_1 \left[(J_{A33} + J_D) - (J_{A22} + J_D) \right]$
J_{11}	$= N_g^2 \, J_{MR} + J_{A11} + J_D$
J_{33}	$= N_g^2 \, J_{MR} + J_{c33} + (J_{A33} + J_D) \cos^2 \delta_1$ $+ (J_{A22} + J_R) \sin^2 \delta_1$

J_R $\triangleq$ polar moment of inertia of the CMG wheel about the $\bar{1}_{2A}$ vector

J_D $\triangleq$ polar moment of inertia of the wheel about an axis perpendicular to the $\bar{1}_{2A}$ vector

J_{A11}, J_{A22}, J_{A33} $\triangleq$ polar moment of inertia of the inner gimbal exclusive of the wheel about the $\bar{1}_{1A}$, $\bar{1}_{2A}$, $\bar{1}_{3A}$ vectors, respectively

J_{C33} $\triangleq$ polar moment of inertia of the outer gimbal about the $\bar{1}_{3C}$ vector

J_{MR} $\triangleq$ polar moment of inertia of the torque motor rotor about its rotational axis

K_{SL} gain constant

$\overline{M}_R$ reaction moment of the CMG's on the base of the vehicle

N_g gear ratio of the gimbal drives

p Laplace operator

s $\triangleq$ sine

$\delta_{1(j)}$ inner gimbal angle of the (j) CMG

$\delta_{3(j)}$ outer gimbal angle of the (j) CMG

$\dot{\delta}_{1(j)}$, $\dot{\delta}_{3(j)}$ time rate of change of angles $\delta_{1(j)}$, $\delta_{3(j)}$

$\dot{\delta}_{1(com)(j)}$, $\dot{\delta}_{3(com)(j)}$ input commands to the inner and outer gimbal velocity servos of the (j) CMG

$\overline{\omega}_{VA(j)}$ actual inner gimbal rate of the (j) CMG with respect to vehicle space

DEFINITION OF SYMBOLS (Concluded)

$\bar{\omega}_{1C1C}$, $\bar{\omega}_{1C2C}$ components of vector $\bar{\omega}_{1C}$ along the coordinates $\bar{1}_{1C}$, $\bar{1}_{2C}$

$\bar{\omega}_{1B3B}$ $\bar{1}_{3B}$ component of the $\bar{\omega}_{1B}$ vector

$\bar{1}_{iA(j)}$ coordinate system of the "A"$_{(j)}$ space or the inner gimbal space of the jth CMG. In "A" space, the inner gimbal rotates about the $\bar{1}_{1A(j)}$ axis. The spin axis corresponds to $\bar{1}_{2A(j)}$, and $\bar{1}_{3A(j)}$ forms the third coordinate of a right-hand orthogonal system.

AN IMPROVED CONTROL SYSTEM FOR THE APOLLO TELESCOPE MOUNT

SUMMARY

A different method of operating the present control system for the Apollo Telescope Mount's control moment gyro is presented. This method results in a broader bandwidth for the control system and consists of modifying the double-gimbal control moment gyros to operate in a single-gimbal mode during all solar experimental periods. If the inner gimbals are used for dynamic control, then the outer gimbals would be inhibited or rigidly clamped to the frame during the experiments. Between experiments, the inhibited outer gimbals would be oriented to maximize the momentum storage capability of the system. The expected increase in bandwidth is from two to three times the present system bandwidth. Inner to outer gimbal cross coupling nonlinearities would also be eliminated during experimental periods. The H-vector control law would still be applicable for this new configuration.

INTRODUCTION

The present attitude control system for the Apollo Telescope Mount (ATM) utilizes three double-gimbal control moment gyros (CMG's) [1] for momentum exchange. The three double-gimbal CMG, or six-pac [2], configuration provides 100 percent utilization of the total momentum available for all three axes with comparatively low power consumption. It also provides 100 percent redundancy of the total control, so adequate attitude control to conduct solar experiments can be maintained with one CMG completely inoperative.

The improved attitude control (IAC) system for the ATM, outlined in this report, will not compromise any of the advantages of the present control system. Moreover, the IAC system will improve the present control system in at least three ways.

1. A wider dynamic range of at least double the present bandwidth is provided.

2. Some nonlinearities resulting from gimbal cross coupling are eliminated.

3. A potential stability problem arising from gimbal cross coupling is deterred.

The basic idea of the IAC system is to use only one set of gimbals of the double-gimbal CMG's for the dynamic attitude control of the ATM. If the inner gimbals are used for dynamic control, the outer gimbals would be clamped rigidly to the frame during all solar experimental periods. Between experiments the outer gimbals would be positioned to obtain optimum utilization of the stored momentum of the CMG six-pac configuration. This report presents only an outline of the IAC system to disseminate the idea. Of course, many details remain to be worked out before such a system could be implemented.

Test data that show the increase in bandwidth to be expected using the IAC system are given. Elimination of the gimbal cross coupling is illustrated and a control law for use with this system is described.

DYNAMIC TEST DATA

The CMG dynamic test data presented here were taken by the Bendix Corporation, Teterboro, New Jersey [3]. The test data included transient responses and steady-state variable frequency responses. The standard test conditions were given as follows:

1. Linear and desaturation resolver excitations were removed.

2. Accelerometers were disconnected.

3. All unused inputs were shorted.

4. Electronic crossfeed compensation was in use, unless otherwise noted.

5. The test stand had a single point ground.

Because of the nonlinearities in the CMG, the steady-state dynamic test data do not yield a true frequency response. The data plotted in Reference 3 are the ratio of the peak output signal to the peak input signal. The amplitude frequency "portraits" for two tests are shown in Figure 1. For both tests the momentum wheel was at rated speed, and the inner gimbal rate loop was driven with a 20.0 volt peak-to-peak sinusoidal signal into the distributive law input (attenuation = 0.230) to produce a gimbal rate input of 4.6 deg/sec peak-to-peak. Curve A is for test 3A3, conducted with the inner gimbal at +45 deg and the outer gimbal at 0 deg. Curve B is for test 3A4, conducted with the inner gimbal at +45 deg and the outer gimbal clamped to the frame at 0 deg.

It is quite apparent from the response data of these two tests that clamping or holding the outer gimbal increases the dynamic range of the CMG. A table in Reference 3 gives the dynamic range or bandwidth of the CMG as 2.5 Hz for test 3A3 (Curve A) and 5.9 Hz for test 3A4 (Curve B), using tachometer measurements, and 2.8 Hz for test 3A3 and 9.2 Hz for test 3A4, using data from the torque measuring fixture (TMF). By clamping the outer gimbal to the frame, the bandwidth is increased between two to three times over its value when the outer gimbal is not clamped.

The only difference between test 3A3 and test 3A4 is the clamping of the gimbal to the frame; therefore, it can be assumed that the variation in bandwidth is due primarily to gimbal cross coupling. It is possible that the variation in bandwidth noted in this report is accentuated by the presence of backlash in the gimbal drives. The use of antibacklash gear trains for the gimbal drives might diminish the bandwidth variation, but it will not eliminate the gimbal cross coupling.

GIMBAL CROSS COUPLING

The dynamics of the inner and outer gimbals can be expressed in a simplified manner as

$$\left(pJ_{11} + N_g \, G_1 \right) \dot{\delta}_1 - \left(H \cos \delta_1 - G_{cc(1)} \right) \dot{\delta}_3 = N_g \, G_1 \, \dot{\delta}_{1(com)} - pJ_1 \, \omega_{1C1C}$$

$$- H \sin \delta_1 \, \omega_{1C2C} + H \cos \delta_1 \, \omega_{1B3B} \tag{1}$$

and

$$\left(H \cos \delta_1 - G_{cc(3)}\right)\dot{\delta}_1 + \left(pJ_{33} + N_g G_3\right)\dot{\delta}_3 = N_g G_3 \dot{\delta}_{3(com)} - H \cos \delta_1 \, \omega_{1C1C}$$

$$- pJ_3 \, \omega_{1C2C} - pJ_2 \, \omega_{1B3B} \quad .$$

$$(2)$$

These equations do not account for the compliance of the gimbals, the gimbal drives, nor nonlinearities caused by backlash in the gimbal drives, bearing friction, etc.

The signal flow graph for equations (1) and (2) was derived in a report by Morine and O'Connor [2]; a modified version is shown in Figure 2. The solid branches in Figure 2 represent kinematic terms, and the dashed branches represent the electrical portion of the gimbal velocity servos. The individual terms are defined in the list of symbols.

If only a single input signal into the CMG of Figure 2 is considered, and that signal is $\dot{\delta}_{1(com)}$, then the transfer function between the input and the inner gimbal response is

$$\frac{\dot{\delta}_1}{\dot{\delta}_{1(com)}} = \frac{N_g G_1 \left(pJ_{33} + N_g G_3\right)}{\Delta} \quad (3)$$

where

$$\Delta = \left[\left(pJ_{11} + N_g G_1\right)\left(pJ_{33} + N_g G_3\right) + \left(H \cos \delta_1 \right.\right.$$

$$(4)$$

$$\left.\left. - G_{cc(1)}\right)\left(H \cos \delta_1 - G_{cc(3)}\right)\right] \quad .$$

The characteristic equation of the CMG is Δ, and it is obtained from equations (1) and (2). Dividing the numerator and denominator of equation (3) by J_{33} gives
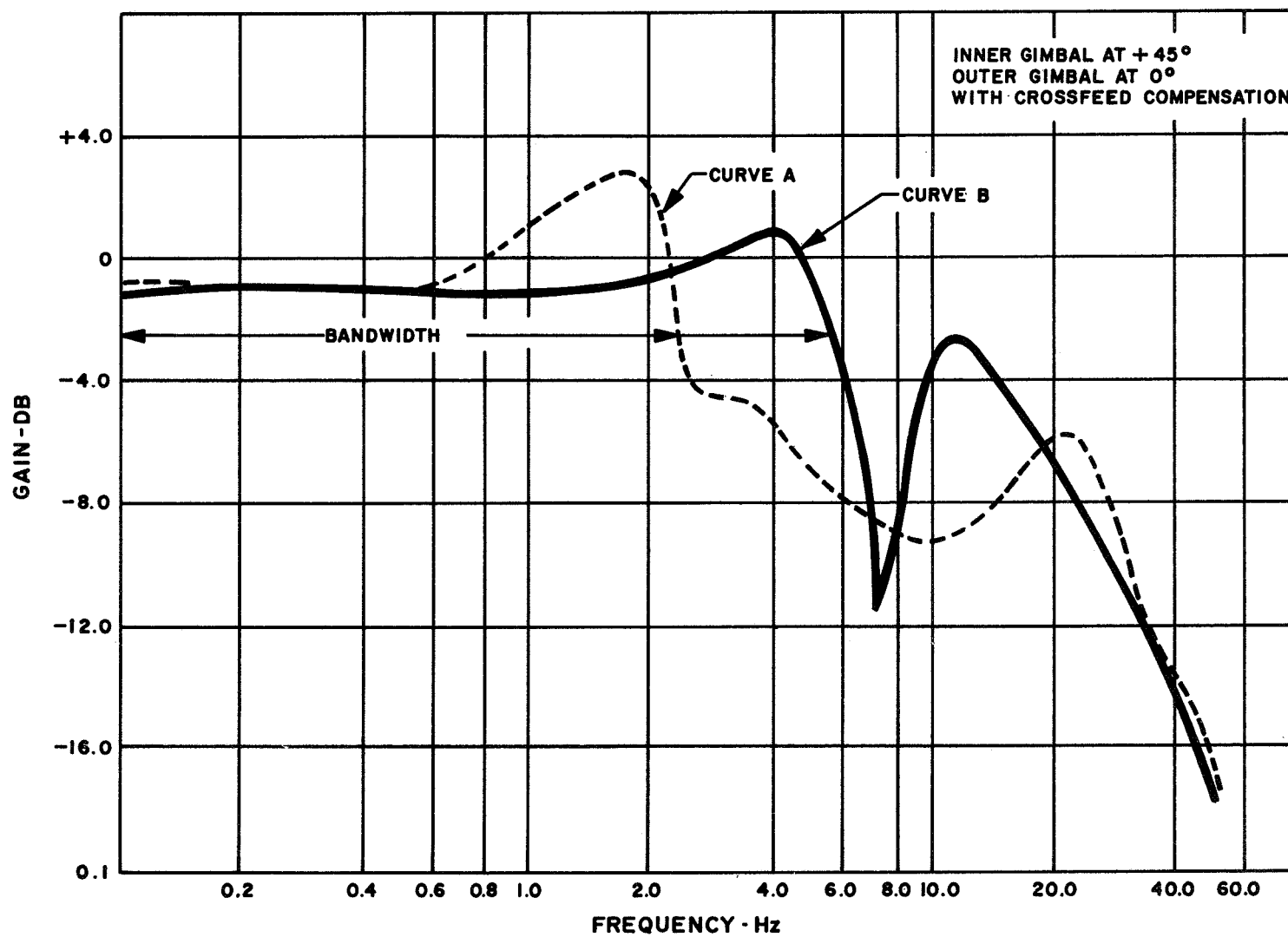
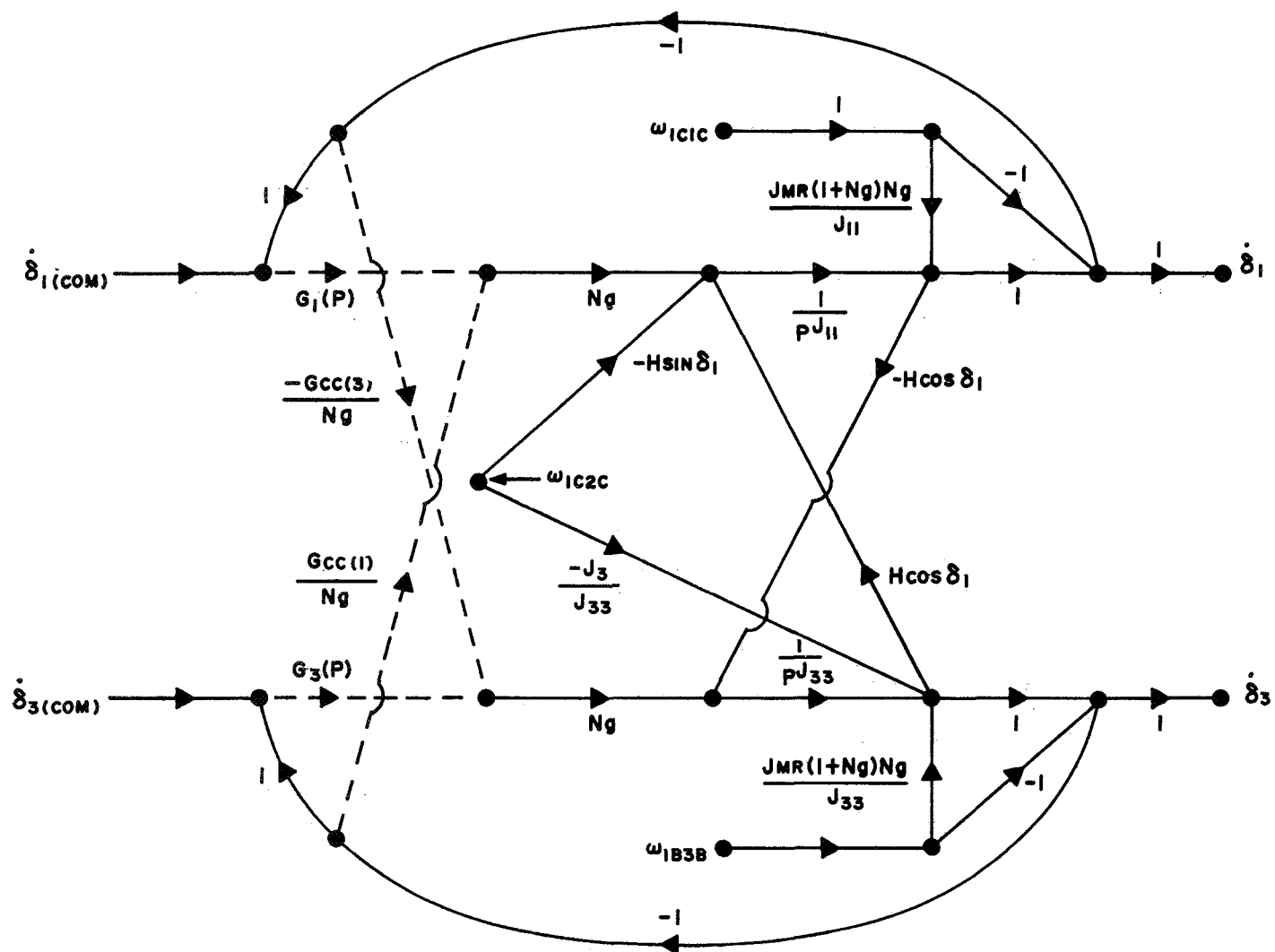FIGURE 1. AMPLITUDE FREQUENCY CHARACTERISTICS OF A DOUBLE-GIMBAL CMG

FIGURE 2.   A SIGNAL FLOW GRAPH OF A CMG

$$\frac{\dot{\delta}_1}{\dot{\delta}_{1(com)}} = \frac{N_g G_1 \left(p + \frac{N_g G_3}{J_{33}} \right)}{(pJ_{11} + N_g G_1)\left(p + \frac{N_g G_3}{J_{33}} \right) + \left[\frac{\left(H \cos \delta_1 - G_{cc(1)} \right)}{1} \cdot \frac{\left(H \cos \delta_1 - G_{cc(3)} \right)}{J_{33}} \right]} \tag{5}$$

By clamping the outer gimbal to the frame, the outer gimbal inertia, contained in the term J_{33}, becomes extremely large; therefore, we can write

$$\frac{N_g G_3}{J_{33}} \rightarrow 0 \tag{6}$$

and

$$\frac{\left(H \cos \delta_1 - G_{cc(1)} \right)\left(H \cos \delta_1 - G_{cc(3)} \right)}{J_{33}} \rightarrow 0 \quad . \tag{7}$$

Applying these two relations to equation (5) and simplifying yields

$$\frac{\dot{\delta}_1}{\dot{\delta}_{1(com)}} = \frac{1}{1 + p \frac{J_{11}}{N_g G_1}} \tag{8}$$

The transfer function of equation (8) can be obtained from the signal flow graph of Figure 2 if the gimbal cross coupling branches are eliminated; this is the desired objective of the IAC system.

The clamping of the outer gimbal to the frame probably can be accomplished best by mechanical means; for instance, by an electromagnetic brake. Locking the outer gimbal torquer on the present ATM/CMG configuration will not be adequate because of the compliance of the associated gear train. The outer gimbal itself must be clamped to ensure that it will have zero velocity with respect to its mounting base.

IAC SYSTEM CONTROL LAW

The primary objective of the IAC system is to increase the bandwidth of the ATM/CMG control system. It was assumed that a minimum amount of

modifications to existing hardware would be desirable while achieving the stated objective. A cursory examination shows that the H-vector control law of the present ATM/CMG configuration can be used for the IAC system. Furthermore, using the present H-vector control law simplifies the redundancy operation requirements. In future applications involving double-gimbal CMG's, it would be desirable to investigate other control laws to determine the one most suitable for use with the IAC system.

Since there is only one gimbal velocity servo per CMG to provide the necessary momentum control, the steering law for the IAC system is simpler than for the present control system. This can be shown as follows: the cross-product steering law for the jth CMG of the present ATM/CMG control system [2] is given as

$$\bar{\omega}_{VA(j)} = K_{SL} \left[\bar{1}_{2A(j)} \times \overline{H}_{TE} \right] \quad , \text{ (j) CMG} \tag{9}$$

where $\overline{H}_{TE}$ is the total error momentum. It can be expressed in the inner gimbal coordinate space as

$$\overline{H}_{TE} = \sum_{i=1}^{3} \left[\bar{1}_{iA(j)} \, H_{TEiA(j)} \right] \quad , \text{ j = 1, 2, 3} \quad . \tag{10}$$

Substituting equation (10) into equation (9) and performing the indicated vector multiplication gives the angular velocity of the inner gimbal, or

$$\bar{\omega}_{VA(j)} = K_{SL} \left[\bar{1}_{1A(j)} \, H_{TE3A(j)} - \bar{1}_{3A(j)} \, H_{TE1A(j)} \right] \quad . \tag{11}$$

For the IAC system, the angular velocity of the inner gimbal can be given in terms of the inner gimbal angle rate, or

$$\bar{\omega}_{VA(j)} = \bar{1}_{1A(j)} \, \dot{\delta}_{1(j)} \tag{12}$$

for the jth CMG. If the inner gimbal angle rate signal is chosen as

$$\dot{\delta}_{1(j)} = K_{SL} \, H_{TE3A(j)} \tag{13}$$

and, if this value of $\dot{\delta}_{1(j)}$ is substituted into equation (12), the angular velocity of the inner gimbal is then expressed as

$$\bar{\omega}_{VA(j)} = K_{SL} \, \bar{1}_{1A(j)} \, H_{TE3A(j)} \tag{14}$$

Thus, the steering law for the IAC system given by equation (14) is seen to have the same terms as the first term of the cross-product steering law given in equation (11). The gain term K_{SL} of equation (14) will, of course, be a different value than the gain term K_{SL} of equation (11).

To find the resulting moment on the ATM cluster caused by the steering law of equation (14), we first express the reaction moment equation as

$$\bar{M}_{R} = - \frac{d\bar{H}_{T}}{dt_{V}} = - \sum_{j=1}^{3} \bar{\omega}_{VA(j)} \times \bar{H}_{(j)} \tag{15}$$

where

$$\bar{H}_{(j)} = H \, \bar{1}_{2A(j)} \tag{16}$$

If equations (14) and (16) are substituted into equation (15) and the indicated vector multiplication is performed, the reaction moment is given as

$$\frac{d\bar{H}_{T}}{dt_{V}} = K_{SL} \, H \sum_{j=1}^{3} \bar{1}_{3A(j)} \, H_{TE3A(j)} \tag{17}$$

For the six-pac configuration, therefore, the IAC system will provide three axis control moments except for the so-called parallel or antiparallel condition, discussed later in this section.

To show the relationship between the error momentum in vehicle coordinate space to that in inner gimbal space requires the use of several transformations. For the six-pac configuration, the transformation of the error momentum from vehicle coordinates into CMG base coordinates is given by equations (18) through (20).

$$
\begin{bmatrix} H_{TE1B(1)} \\ H_{TE2B(1)} \\ H_{TE3B(1)} \end{bmatrix} = \begin{bmatrix} 0 & 1 & 0 \\ 1 & 0 & 0 \\ 0 & 0 & -1 \end{bmatrix} \begin{bmatrix} H_{TEX} \\ H_{TEY} \\ H_{TEZ} \end{bmatrix} , \quad (1) \text{ CMG} \qquad (18)
$$

$$
\begin{bmatrix} H_{TE1B(2)} \\ H_{TE2B(2)} \\ H_{TE3B(2)} \end{bmatrix} = \begin{bmatrix} 0 & 0 & 1 \\ 0 & 1 & 0 \\ -1 & 0 & 0 \end{bmatrix} \begin{bmatrix} H_{TEX} \\ H_{TEY} \\ H_{TEZ} \end{bmatrix} , \quad (2) \text{ CMG} \qquad (19)
$$

$$
\begin{bmatrix} H_{TE1B(3)} \\ H_{TE2B(3)} \\ H_{TE3B(3)} \end{bmatrix} = \begin{bmatrix} 1 & 0 & 0 \\ 0 & 0 & 1 \\ 0 & -1 & 0 \end{bmatrix} \begin{bmatrix} H_{TEX} \\ H_{TEY} \\ H_{TEZ} \end{bmatrix} , \quad (3) \text{ CMG} \quad . \qquad (20)
$$

The transformation matrix from the CMG base coordinates into inner gimbal coordinates of any of the three CMG's is given as

$$
\begin{bmatrix} H_{TE1A(j)} \\ H_{TE2A(j)} \\ H_{TE3A(j)} \end{bmatrix} = \begin{bmatrix} c\delta_{3(j)} & s\delta_{3(j)} & 0 \\ -s\delta_{3(j)}\, c\delta_{1(j)} & c\delta_{3(j)}\, c\delta_{1(j)} & s\delta_{1(j)} \\ s\delta_{3(j)}\, s\delta_{1(j)} & -c\delta_{3(j)}\, s\delta_{1(j)} & c\delta_{1(j)} \end{bmatrix} \begin{bmatrix} H_{TE1B(j)} \\ H_{TE2B(j)} \\ H_{TE3B(j)} \end{bmatrix} \tag{21}
$$

The error momentum component used to produce a reaction moment can now be expressed in terms of inner gimbal space as

$$
\overline{H}_{TE3A(1)} = s\delta_{3(1)}\, s\delta_{1(1)}\, H_{TEY} - c\delta_{3(1)}\, s\delta_{1(1)}\, \overline{H}_{TEX} - c\delta_{1(1)}\, \overline{H}_{TEZ} \tag{22}
$$

$$
\overline{H}_{TE3A(2)} = s\delta_{3(2)}\, s\delta_{1(2)}\, \overline{H}_{TEZ} - c\delta_{3(2)}\, s\delta_{1(2)}\, \overline{H}_{TEY} - c\delta_{1(2)}\, \overline{H}_{TEX} \tag{23}
$$

$$
\overline{H}_{TE3A(3)} = s\delta_{3(3)}\, s\delta_{1(3)}\, \overline{H}_{TEX} - c\delta_{3(3)}\, s\delta_{1(3)}\, \overline{H}_{TEZ} - c\delta_{1(3)}\, \overline{H}_{TEY} \tag{24}
$$

Thus, the reaction moment from each CMG is dependent on the gimbal angles of both the inner and outer gimbals and the error momentum components expressed in the vehicle coordinate axes. For the initial conditions, where $\delta_{3(j)} = +45$ deg and $\delta_{1(j)} = 0$ deg, the error momentums along the $\overline{i}_{3A(j)}$ axes are

$$
\overline{H}_{TE3A(1)} = -\overline{H}_{TEZ} \quad , \quad (1) \ CMG \tag{25}
$$

$$
\overline{H}_{TE3A(2)} = -\overline{H}_{TEX} \quad , \quad (2) \ CMG \tag{26}
$$

$$
\overline{H}_{TE3A(3)} = -\overline{H}_{TEY} \quad , \quad (3) \ CMG \tag{27}
$$

For other gimbal orientations the error momentum will be composed of X, Y, and Z components as shown in equations (22) through (24).

The implementation of the IAC system for the gimbal velocity servos of a single CMG is shown in Figure 3. The associated resolver chains used to obtain the error momentum in terms of the inner gimbal coordinates would be the same as in the present configuration [2]. The digital computer will determine the outer gimbal angles $\delta_{3(j)}$ necessary to optimize the utilization of the stored momentum.

It has been shown by Kennel [4] that the most desirable orientation of the CMG momentum vectors is obtained with the isogonal distribution law; that is, the individual angular momentum vectors for each CMG contribute an equal component to the total momentum vector. This condition results when the angles between the individual momenta are equal and the angles between the individual momenta and the total momentum vector are also equal. This orientation avoids the parallel and antiparallel conditions, maximizes the attitude gain available, and minimizes the cross coupling. The IAC system appears to be completely compatible with the isogonal distribution law. At the end of a solar experiment, the desired outer gimbal angles would be determined based on the then existing inner and outer gimbal angles. The outer gimbals would then be commanded to their new orientation while the inner gimbals assumed their new positions by maintaining the desired attitude of the space station. The reorientation of the outer gimbal angles will appear like a programed disturbance, the character of which can be determined to provide a minimum of spacecraft attitude error.

CONCLUSIONS

The bandwidth of the CMG used for the Apollo Telescope Mount can be increased by a factor of at least two by clamping the outer gimbal rigidly to its frame. This modification to the present ATM/CMG control system, as presented in this report, does not compromise any of its existing advantages. Clamping of the outer gimbal also eliminates the inner-outer gimbal cross coupling, and, with antibacklash gimbal drives, a more realistic linear stability analyses of the control system would be possible.
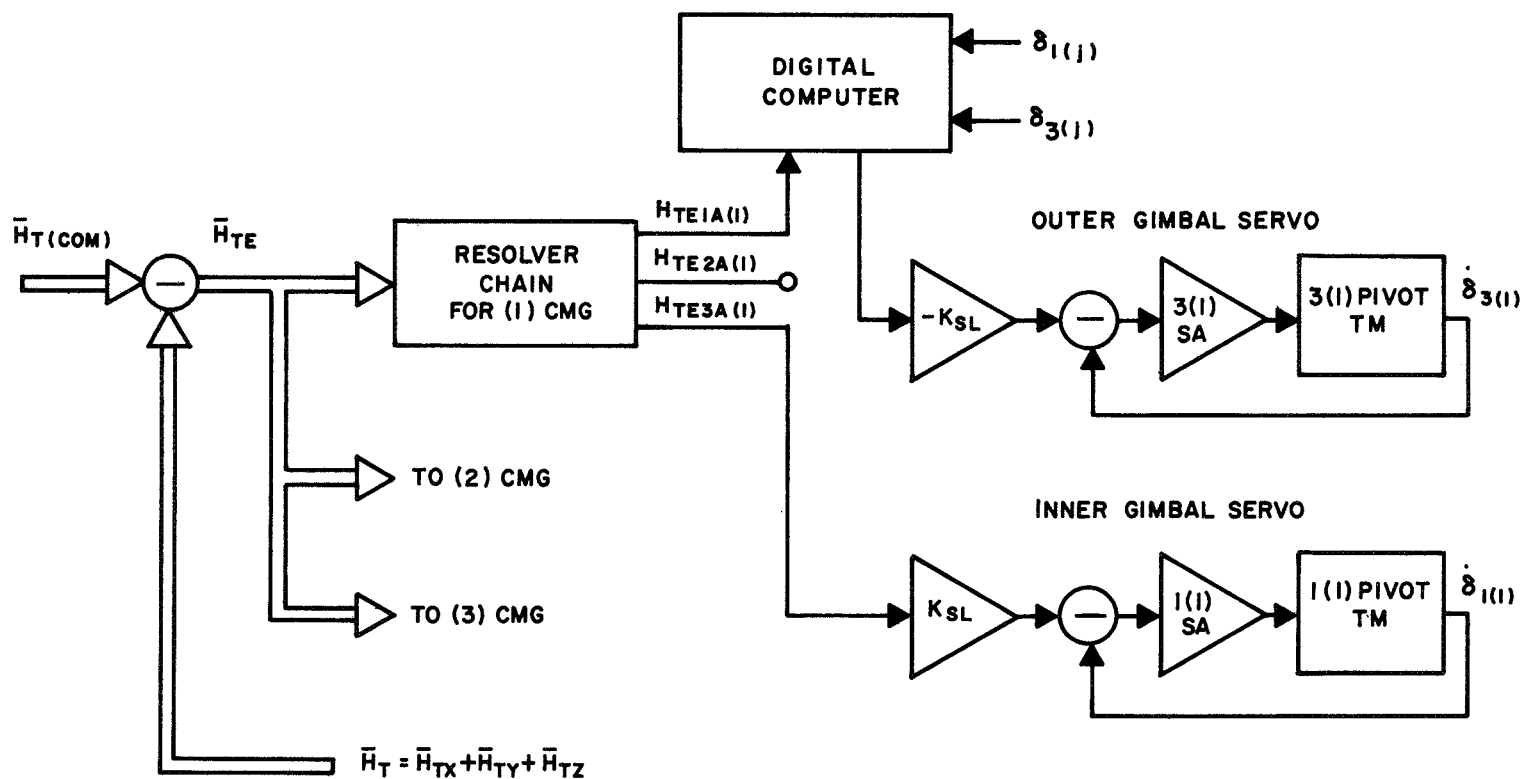
FIGURE 3. GIMBAL VELOCITY SERVO BLOCK DIAGRAM FOR THE IAC SYSTEM

REFERENCES

1. Chubb, W. B.; Schultz, D. N.; and Seltzer, S. M.: Attitude Control and Precision Pointing of the Apollo Telescope Mount. AIAA Guidance, Control, and Flight Dynamics Conference, Huntsville, Ala., Paper 67-534, Aug. 1967.

2. O'Connor, B. J.; and Morine, L. A.: Description of the CMG and Its Application to Space Vehicle Control. AIAA Guidance, Control, and Flight Dynamics Conference, Huntsville, Ala., Paper 67-550, Aug. 1967.

3. Bertini, J.; and DeFonzo, R. J.: Preliminary Test Results ATM-CMG Servo Loops. Engineering File – MT-15,428, The Bendix Corporation, Navigation and Control Division, Teterboro, N. J., May 6, 1968.

4. Kennel, H. F.: Individual Angular Momentum Vector Distribution and Rotation Laws for Three Double-Gimbaled Control Moment Gyros. NASA TM X-53696, Jan. 22, 1968.

AN IMPROVED CONTROL SYSTEM FOR THE
APOLLO TELESCOPE MOUNT

By M. T. Borelli

The information in this report has been reviewed for security classification. Review of any information concerning Department of Defense or Atomic Energy Commission programs has been made by the MSFC Security Classification Officer. This report, in its entirety, has been determined to be unclassified.

This document has also been reviewed and approved for technical accuracy.

H. H. HOSENTHIEN
Chief, R&D Analysis Office

F. B. MOORE
Director, Astrionics Laboratory

DISTRIBUTION

INTERNAL (Concluded)   EXTERNAL

S&E-ASTR-G   Scientific and Technical Information
    Mr. Caudle   Facility (2)
    Mr. Davis   P. O. Box 33
    Mr. Golley   College Park, Maryland 20740
    Mr. Drawe   ATTN: NASA Representative (S-AK/RKT)

S&E-ASTR-I   Martin-Marietta Corp.
    Mr. Duggan   Denver Division (3)
                                        P. O. Box 179
S&E-ASTR-M   Denver, Colorado 80201
    Mr. Counter   ATTN: Mr. T. Glahn

S&E-ASTR-S   Bendix Corp.
    Mr. Gassaway   Navigation and Control Division (9)
    Mr. Wood   Teterboro, New Jersey 07608
    Mr. Thompson   ATTN: Mr. L. Morine, Dept. 7511
    Mr. Brooks
    Mr. Blanton   NASA-Langley Research Center (5)
    Mr. Chubb (5)   Langley Field
    Mr. Nicaise (5)   Hampton, Virginia 23365
    Mr. Schultz (5)   ATTN: Dr. Kurzhals
    Mr. Gilino
    Mr. Shelton (3)   Bendix Corp.
                                        Navigation and Control Division (4)
S&E-ASTR-C   Research Blvd.
    Mr. Swearingen (3)   Madison, Alabama 35758
    Mr. Bridges   ATTN: Mr. E. Hahn

A&TS-PAT   Bendix Research Laboratories (2)
    Mr. Wofford   10 1/2 Mile Road
                                        Southfield, Michigan 48075
A&TS-MS-H   ATTN: Mr. B. K. Powell

A&TS-MS-IP (2)   Bendix Research Laboratories
                                        Denver Facility (5)
A&TS-MS-IL (8)   2796 S. Federal Blvd.
                                        Denver, Colorado 80236
A&TS-MS-T (6)   ATTN: Mr. R. Duncan

I-RM-M   Lockheed Missiles and Space Co. (5)
                                        Sunnyvale, California 94000
                                        ATTN: Dr. Dale Ingwerson/Dr. S. Seltzer

EXTERNAL (Concluded)

Lockheed Missiles and Space Co. (2)
Research Park
Huntsville, Alabama 35805
ATTN: Dr. W. Trautwein

Bellcomm, Inc. (2)
1100 17th Street, NW
Washington, D. C. 20036
ATTN: Mr. J. Kranton

Manned Spacecraft Center
National Aeronautics and Space Administration
Houston, Texas 77058
ATTN: Mr. F. Coe, CF 23 (2)
　　　　Col. G. Cooper, CB
　　　　Dr. O. Garriott, CB
　　　　Dr. E. Gibson, CB
　　　　Mr. W. Hamby, KM
　　　　Mr. F. Littleton, KM
　　　　Mr. R. Machell, KF
　　　　Mr. O. Smith, KF

Martin-Marietta Corp.
P. O. Box 3040
Huntsville, Alabama 35810
ATTN: Mr. C. Langford

Sperry Rand Corp.
Space Support Division (4)
716 Arcadia Circle
Huntsville, Alabama 35801
ATTN: Mr. J. Faison

Sperry Rand Corp.
Flight Systems Division
21111 North 19th Avenue
Phoenix, Arizona 85027
ATTN: Dr. R. E. Andeen (4)